Polyhedron 33 (2012) 289–296

Contents lists available at SciVerse ScienceDirect

Polyhedron

journal homepage: www.elsevier.com/locate/poly

Coordination studies of copper(II), cobalt(II) and iron(II) with isomeric pyridyl–tetrazole ligands

Andrew D. Bond [a], Adrienne Fleming [b], Jackie Gaire [b], Fintan Kelleher [b], John McGinley [c,*], Vickie McKee [d], Ursula Sheridan [c]

[a] Department of Physics and Chemistry, University of Southern Denmark, DK-5230 Odense M, Denmark
[b] Molecular Design and Synthesis Group, Department of Science, Institute of Technology Tallaght, Dublin 24, Ireland
[c] Department of Chemistry, National University of Ireland Maynooth, Maynooth, Co. Kildare, Ireland
[d] Department of Chemistry, Loughborough University, Loughborough, Leicestershire LE11 3TU, UK

ARTICLE INFO

Article history:
Received 11 October 2011
Accepted 21 November 2011
Available online 28 November 2011

Keywords:
Coordination chemistry
Transition metal
Pyridyl–tetrazole ligand
X-ray crystal structures

ABSTRACT

The reaction of 2-(2H-tetrazol-5-yl)pyridine (**L1**) with 1,6-dibromohexane results in formation of the isomers 2-(6″-bromohexyl)-(1-tetrazol-5-yl)pyridine (**L2**) and 2-(6″-bromohexyl)-(2-tetrazol-5-yl)pyridine (**L3**). Coordination reactions of **L2** and **L3** with $CuCl_2{\cdot}2H_2O$, $Co(SCN)_2$ and $Fe(ClO_4)_2{\cdot}H_2O$ yielded the strongly coloured solids $[Cu(II)(\mathbf{L2})Cl_2]_2$ (**1**), $[Cu(II)(\mathbf{L3})Cl_2]_2$ (**2**), $[Co(II)(\mathbf{L2})_2(NCS)_2]$ (**3**), $[Co(II)(\mathbf{L3})_2(NCS)_2]$ (**4**), $[Fe(II)(\mathbf{L2})_2(H_2O)_2](ClO_4)_2$ (**5**) and $[Fe(II)(\mathbf{L3})_2(H_2O)_2](ClO_4)_2$ (**6**), containing high-spin metal centres for the Co(II) and Fe(II) compounds. X-ray crystal structures were obtained for complexes **1**–**5**. In each complex, ligands **L2** and **L3** coordinate to the metal centre through the pyridyl N atom and the *1-N* site of the tetrazole ring, and the pyridyl–tetrazole ligand remains planar in all cases except **3**. Complexes **1** and **2** comprise a central Cu_2Cl_2 dimeric core with Cu(II) in an essentially square-pyramidal coordination environment. Complexes **3** and **4** contain Co(II) in a distorted octahedral coordination environment. In **3**, the pyridyl and tetrazole rings of **L2** are twisted with respect to each other and the complex adopts a puckered conformation in its equatorial plane. Complex **5** contains water molecules coordinated to Fe(II) in the axial sites, which form hydrogen bonds to the perchlorate counter anions.

1. Introduction

A great deal of attention has been devoted toward the synthesis of functional compounds containing polyazole rings, particularly tetrazoles and their derivatives, due to their practical applications [1–4]. The development of "click" chemistry, as described by Sharpless and co-workers [5], has resulted in a recent increase in tetrazole structures. Tetrazole derivatives have found applications in therapeutics as antihypertensive agents [6], antibiotics [7], and drugs for AIDS treatment [8]. They are also studied in the field of coordination chemistry [9]. Both tetrazole and its derivatives, normally the 5-substituted derivatives, can act as both di- and polydentate ligands exhibiting several coordination modes [10]. Mono 1- and 2-substituted tetrazoles are often used for the construction of coordination networks [9,10]. Our interest in tetrazoles concerns their use as precursors for the formation of new functionalised polytetrazole macromolecules, which have potential applications as sensors or in molecular recognition. We have previously reported the addition of pendant short-chain arms to various bis-tetrazoles, as well as the synthesis of several tetra-tetrazole macrocycles, including the first example of a host–guest interaction between a tetra-tetrazole macrocycle and a solvent molecule [11–16]. To expand this area, we are investigating the use of tetrazole containing compounds as potential metal-based therapeutic agents, especially as anti-cancer or anti-fungicidal agents. In this paper, we describe the synthesis of some pyridyl–tetrazole compounds containing bromohexyl pendant arms (see Scheme 1) and examine their coordination chemistry with Fe(II), Co(II) and Cu(II) salts, which are a range of metal cations which the human body can tolerate. The biological studies of these complexes will be discussed in a future paper [17].

2. Results and discussion

2.1. Ligand syntheses and characterisation

Synthesis of 2-(2H-tetrazol-5-yl)pyridine (**L1**) and its subsequent reaction with 1,6-dibromoexane to give the isomers 2-(6″-bromohexyl)-(1-tetrazol-5-yl)pyridine (**L2**) and 2-(6″-bromohexyl)-(2-tetrazol-5-yl)pyridine (**L3**) was carried out as in a manner similar to that described in the literature [18], as shown in Scheme 1. The reaction of sodium azide with 2-cyanopyridine in the presence

* Corresponding author. Tel.: +353 1 708 4615; fax: +353 1 708 3815.
E-mail address: john.mcginley@nuim.ie (J. McGinley).

0277-5387/$ - see front matter © 2011 Elsevier Ltd. All rights reserved.
doi:10.1016/j.poly.2011.11.038

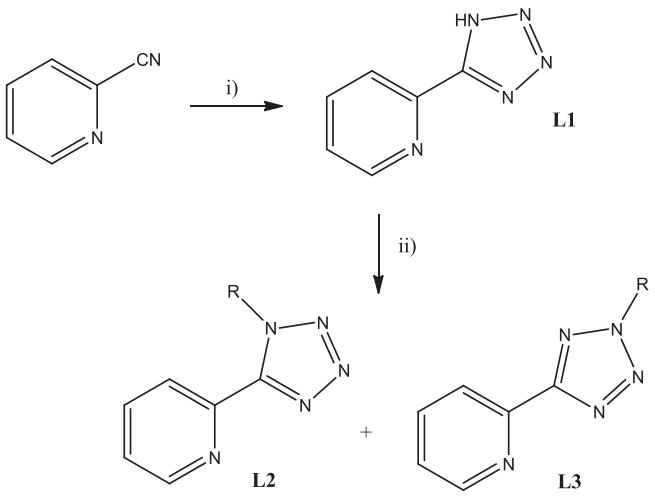

Scheme 1. Reaction conditions: (i) NaN_3, LiCl, NH_4Cl, DMF, Δ, 10 h; (ii) 1,6-dibromohexane, K_2CO_3, butanone, Δ, 24 h; R = $C_6H_{12}Br$.

of ammonium chloride and lithium chloride in dry dimethylformamide (DMF) yielded **L1** as brown needles on recrystallisation from ethanol. The ^{13}C NMR and IR spectra of the needles confirmed the presence of the tetrazole ring with a signal at 154.9 ppm in the ^{13}C NMR spectrum indicating the formation of a 1,5-disubstituted tetrazole and the absence of a signal at 2220 cm^{-1} in the IR spectrum due to an azide band [15,19,20]. The ^1H NMR spectrum of **L1**, obtained in CD_3OD, showed the expected signals for the pyridine ring, while the NH proton on the tetrazole appeared as a broad signal at 3.9 ppm.

The reaction of **L1** with 1,6-dibromohexane in either 2-butanone or acetonitrile with potassium carbonate as base gave a mixture of products **L2** and **L3**, arising from alkylation at either the *1-N* or *2-N* positions. Column chromatography separated the products from the reactants. Both **L2** and **L3** are low melting, waxy solids. The isomers are readily distinguishable by their ^{13}C NMR spectra with the ^{13}C NMR chemical shift of the tetrazole C atom appearing at ca. 154.0 or 164.0 ppm in the 1,5- and 2,5-disubstituted tetrazoles, respectively [15,19,20]. In this case, the *1-N* isomer (**L2**) gave a signal at 151.4 ppm, while the *2-N* isomer (**L3**) gave a signal at 164.7 ppm. The ^1H NMR spectra of both **L2** and **L3** show four signals for the pyridyl protons, a triplet for the methylene group beside the Br atom, a triplet for the methylene group beside the tetrazole and three other signals for the remaining methylene groups of the bromoalkyl chain. The signals for the methylene protons beside the tetrazole appear at 5.00 ppm for **L2** and 4.73 ppm for **L3**.

2.2. Coordination reactions

The transition-metal salts $CuCl_2{\cdot}2H_2O$, $Co(SCN)_2$ and $Fe(ClO_4)_2\times H_2O$ were reacted with **L2** and **L3**, respectively, in methanol at reflux temperature under an inert atmosphere for 2 h. All reactions were carried out using a 1:1 metal:ligand stoichiometry (see Schemes 2 and 3). The resulting strongly coloured solutions were allowed to stand for several days, after which time the solid products were filtered off. Elemental analyses on all of the products obtained showed that the Cu complexes (**1** and **2**) have a 1:1 metal:ligand composition while both the Co complexes (**3** and **4**) and the Fe complexes (**5** and **6**) had a 1:2 metal:ligand composition.

The Cu complexes **1** and **2** have magnetic moments of 2.6 and 3.2 BM, respectively, which indicate the expected presence of Cu(II). Both Co complexes **3** and **4** have magnetic moments in the ranges of 4.5 and 3.65 BM, which are consistent with the presence of high-spin Co(II). The magnetic moments for the Fe complexes **5** and **6** are 4.7 and 5.0 BM, respectively, which indicate the presence of high-spin Fe(II). The observation of high-spin ions in the latter two cases is consistent with the findings of Henderson and co-workers who have reported several complexes of **L1** all contained high-spin Mn(II) [9a].

2.3. Crystal structures of the Cu(II) complexes *1* and *2*

Dark green crystals of **1** and **2** suitable for X-ray diffraction were obtained from methanol and ethanol solutions of $CuCl_2{\cdot}2H_2O$ with **L2** and **L3**, respectively. Crystallographic data for all structures are presented in Table 1. Both **3** and **7** consist of dichloro-bridged dimeric $\{Cu(II)(\mu\text{-}Cl)Cl\}_2$ units, with the coordination sphere about each Cu(II) atom comprising one pyridine N atom, one tetrazole N atom and three Cl atoms (Figs. 1 and 2). Selected bond distances and angles are listed in Tables 2 and 3, respectively. In **1**, the complex lies on a crystallographic inversion centre, while in **2**, the bromohexyl chains adopt different conformations with respect to the central core of the complex. One of the hexyl chains in **2** is disordered (Fig. 2).

The geometry of the central core is closely comparable in **1** and **2**: the 28 non-H atoms in each complex (excluding the bromohexyl chains) can be overlaid with an rms deviation of 0.13 Å. The coordination geometry of each Cu(II) centre is distorted square pyramidal. The Addison parameter, τ, is 0.19 for **1**, compared to 0.05 for Cu(1) and 0.12 for Cu(2), respectively, in **2** (where $\tau = 0$ for ideal square-pyramidal and $\tau = 1$ for ideal trigonal–bipyramidal) [21]. Each pyridyl–tetrazole ligand binds to the Cu(II) atom through one tetrazole N atom at the *1-N* site of the tetrazole ring and through the pyridyl N atom, to generate a five-membered chelate ring. The tetrazole ring is coplanar with the pyridyl ring. This coplanarity has been seen in other metal complexes containing pyridyl–tetrazole ligands [9,10]. In the central core, the four-membered Cu_2Cl_2 rings are planar in both cases, and the Cu(II)–Cl bond distances are comparable to those of other dichloro-bridged dimers in the literature [22]. The Cu–Cl(apical) bond distances are longer than the Cu–Cl(equatorial) bond distances by ca. 0.35 Å (Table 2).

In **1**, the two bromohexyl arms orient themselves above and below the central Cu_2Cl_2 core, pointing away from each other in a centrosymmetric arrangement (Fig. 1), whereas in **2**, both arms point in the same direction (Fig. 2). This difference in orientation is probably attributable to packing effects. In **1**, the complexes are arranged into well-defined layers, with the pyridyl ring of one **L2** ligand approaching the tetrazole ring of an adjacent **L2** ligand in a side-on co-planar fashion, making C–H···N contacts (see Figures in ESI). The bromohexyl arms form an interdigitated arrangement between those layers, with adjacent arms lying parallel to each other in a manner typical of close-packed alkyl chains. In **2**, the comparable side-on approach of **L3** ligands is blocked by the presence of the bromohexyl arm, and the complexes instead adopt a bilayer type arrangement, where the pyridyl ring of one **L3** ligand approaches the Cl atoms of an adjacent complex, making C–H···Cl contacts. In this arrangement, the bromohexyl pendant arms are forced to lie on the same side of the complex, where they form a less well-defined packing pattern between the bilayers.

2.4. Crystal structures of the Co(II) complexes *3* and *4*

Rust-coloured crystals of **3** were obtained from a methanol solution while green crystals of **4** were recrystallised from ethanol. Complex **3** contains one independent molecule lying on a crystallographic inversion centre, while **4** contains two independent complexes, lying on distinct crystallographic inversion centres. Selected bond distances and angles for **3** and **4** are listed in Tables 4 and 5, respectively.

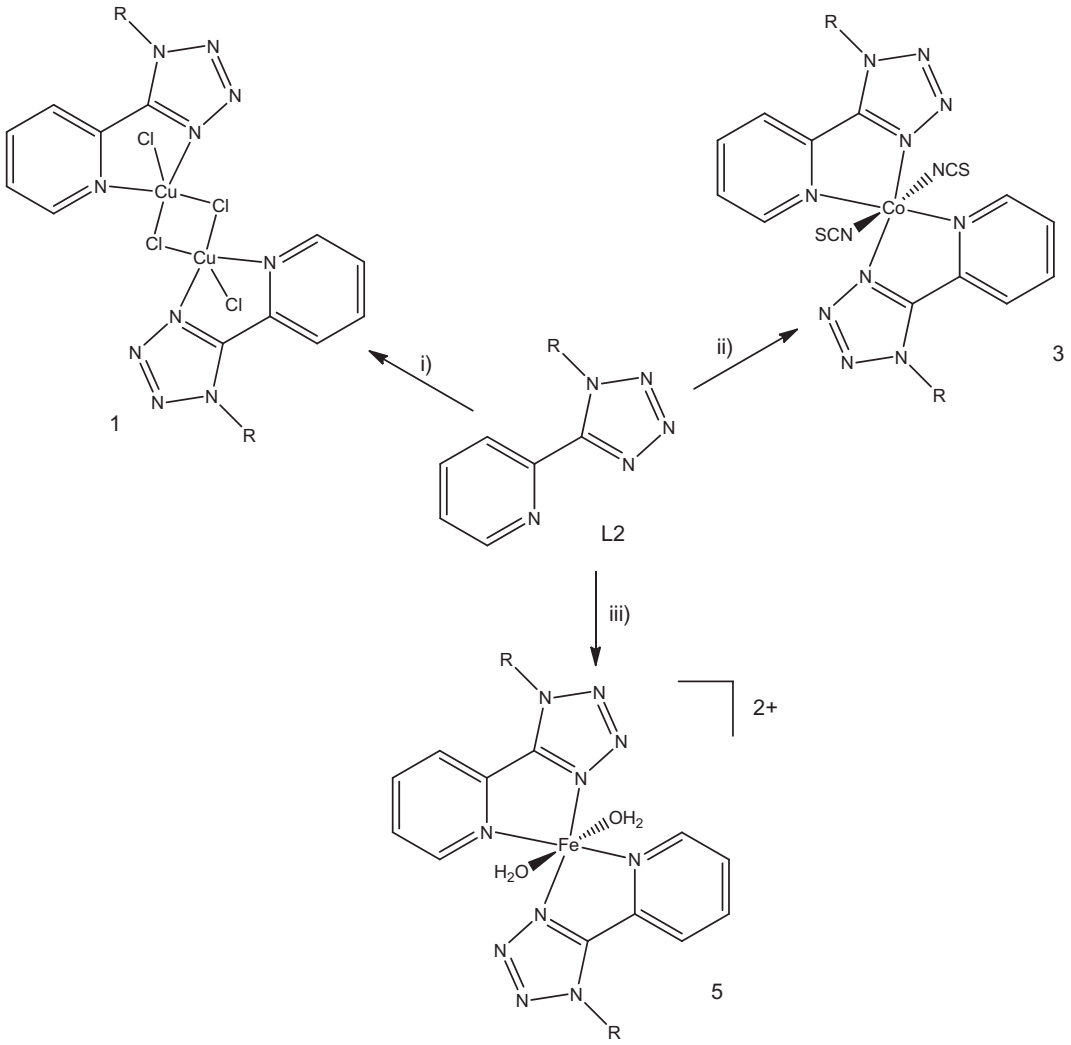

Scheme 2. Reaction conditions: (i) $CuCl_2{\cdot}2H_2O$, MeOH, Δ, 2 h; (ii) $Co(SCN)_2$, MeOH, Δ, 2 h; (iii) $Fe(ClO_4)_2{\cdot}xH_2O$, MeOH, Δ, 2 h.

In both **3** and **4**, Co(II) exhibits an octahedral coordination geometry with the equatorial plane consisting of two pyridyl–tetrazole ligands and the thiocyanate ligands in the axial positions. Again, each pyridyl–tetrazole ligand chelates to Co(II) through one tetrazole N atom at the *1-N* site and through the pyridyl N atom. As for **1** and **2**, the tetrazole rings are coplanar with the pyridine rings in **4**, and the two pyridyl–tetrazole ligands within the complex are also approximately co-planar with each other. In **3**, however, there is a significant twist within the ligand so that the planes of the tetrazole and pyridine rings form dihedral angles of 8.9(1)° and 16.2(1)° in the two independent ligands, and the complex as a whole displays a much more puckered geometry (Fig. 3), reminiscent of the saddle conformation frequently observed in porphyrin complexes. Again, this appears to driven by packing effects. The complexes lie in layers where the equatorial planes of the complexes are all essentially parallel (as opposed to edge-to-face type contacts observed in **4**) (Fig. 5). At one side of the complex, the pyridyl–tetrazole ligands with the smaller degree of twist meet in centrosymmetric face-to-face type contacts. At the other side of the complex, a bromohexyl chain lies across the face of an adjacent complex, and the tetrazole ring of the ligand is twisted away from that chain, giving rise to the larger twist within the ligand. The twist also introduces relatively short N···S contacts to a neighbouring thiocyanate ligand (3.325(4) Å) (Fig. 4).

*2.5. X-ray analysis of the Fe(II) complex of **L2***

Brown crystals of **5** were obtained from the reaction between $Fe(ClO_4)_2{\cdot}H_2O$ and **L2**. Selected bond lengths and angles for **5** are given in Table 6. The complex lies on a crystallographic inversion centre and the bromoalkyl chain is modelled as disordered over two sets of positions (Fig. 6). The Fe(II) centre adopts a slightly distorted octahedral coordination geometry with the pyridyl–tetrazole ligands occupying the equatorial plane and water molecules occupying the axial positions. As for **1**, **2** and **4**, the tetrazole ring is coplanar with the pyridine ring. The complexes lie in layers with the perchlorate counter anions (modelled as disordered) between layers accepting hydrogen bonds from the coordinated water molecules.

3. Experimental

^1H and ^{13}C NMR (δ ppm; *J* Hz) spectra were recorded on a JEOL JNM-LA300 FT-NMR spectrometer using saturated $CDCl_3$ solutions with Me_4Si reference, unless indicated otherwise, with resolutions of 0.18 Hz and 0.01 ppm, respectively. Infrared spectra (cm^{-1}) were recorded as KBr discs or liquid films between KBr plates using a Nicolet Impact 410 FT-IR spectrometer. Melting point analyses were carried out using a Stewart Scientific SMP 1 melting point

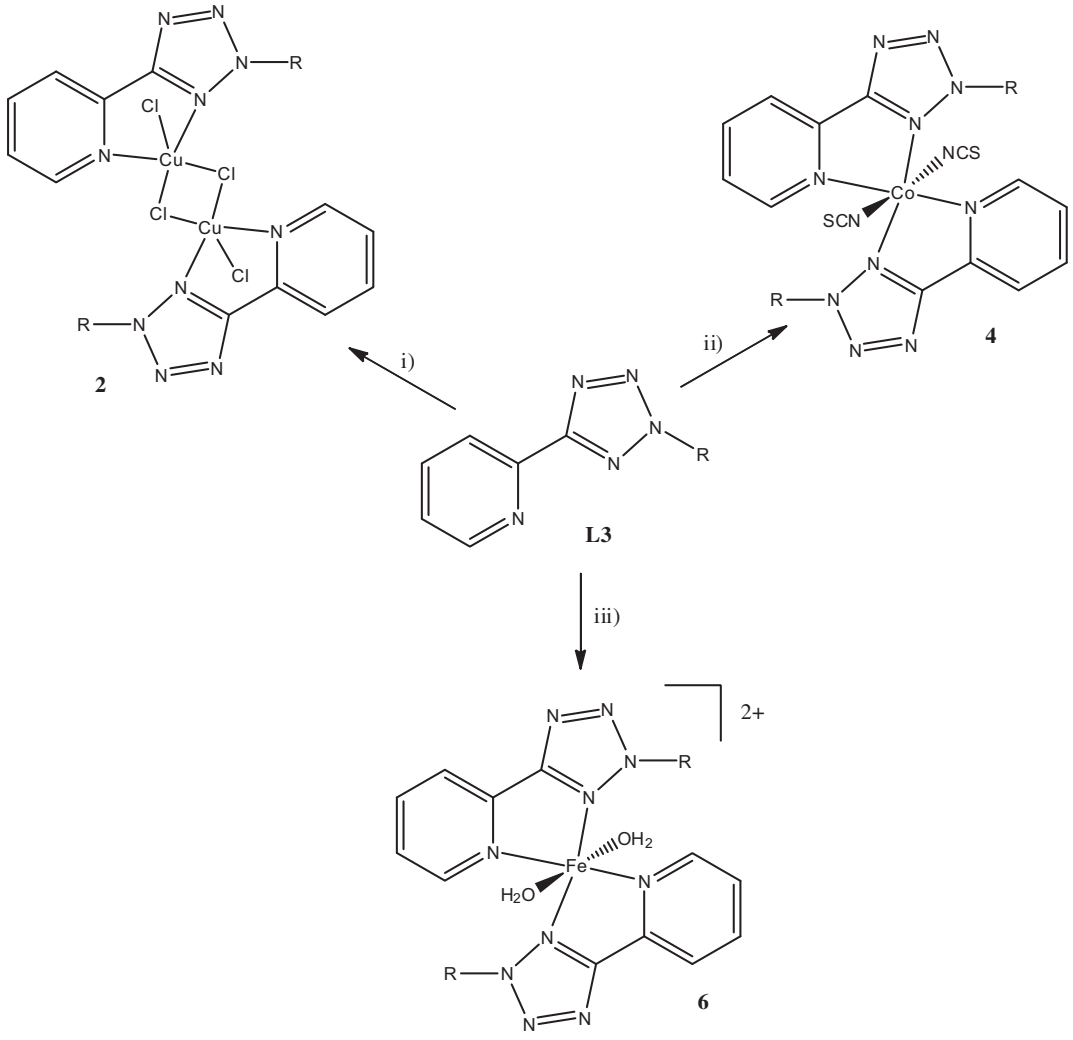

Scheme 3. Reaction conditions: (i) $CuCl_2{\cdot}2H_2O$, MeOH, Δ, 2 h; (ii) $Co(SCN)_2$, MeOH, Δ, 2 h; (iii) $Fe(ClO_4)_2{\cdot}xH_2O$, MeOH, Δ, 2 h.

Table 1
Crystallographic data for **1**–**5**.

	1	**2**	**3**	**4**	**5**
Formula	$C_{24}H_{32}Br_2Cl_4Cu_2N_{10}$	$C_{24}H_{32}Br_2Cl_4Cu_2N_{10}$	$C_{26}H_{32}Br_2CoN_{12}S_2$	$C_{26}H_{32}Br_2CoN_{12}S_2$	$C_{24}H_{36}Br_2Cl_2FeN_{10}O_{10}$
M (g mol^{-1})	889.30	889.30	795.51	795.51	911.20
Crystal system	triclinic	triclinic	triclinic	triclinic	monoclinic
Space group	$P\bar{1}$	$P\bar{1}$	$P\bar{1}$	$P\bar{1}$	$P2_1/c$
T (K)	180(2)	150(2)	120(2)	150(2)	150(2)
a (Å)	9.2946(5)	9.5645(17)	8.7827(4)	8.2324(15)	9.8682(11)
b (Å)	9.4441(7)	12.213(2)	12.1112(6)	12.863(2)	11.7061(12)
c (Å)	10.6132(7)	14.688(3)	16.0963(6)	15.951(3)	15.2784(16)
α (°)	76.945(2)	92.214(3)	83.204(2)	99.917(3)	90
β (°)	80.052(2)	107.256(2)	83.219(2)	93.901(3)	92.999(2)
γ (°)	66.114(2)	93.937(2)	74.195(2)	90.270(3)	90
V (Å^3)	826.35(9)	1631.5(5)	1629.23(13)	1659.8(5)	1762.5(3)
Z	1	2	2	2	2
D_{calc} (g cm^{-3})	1.787	1.810	1.622	1.592	1.717
Reflections collected	14734	13771	32290	12805	14802
Unique reflections	2897	6383	6043	5600	3463
R_{int}	0.026	0.050	0.033	0.067	0.041
Observed reflections [$I > 2(I)$]	2632	3783	4855	2764	2565
Number of parameters	190	415	398	426	319
Number of restraints	0	147	0	468	218
R_1 [$I > 2\sigma(I)$]	0.0264	0.066	0.041	0.081	0.047
wR_2 (all data)	0.074	0.217	0.108	0.252	0.115
Goodness-of-fit (GOF) on F^2	1.09	1.03	1.04	1.05	1.05

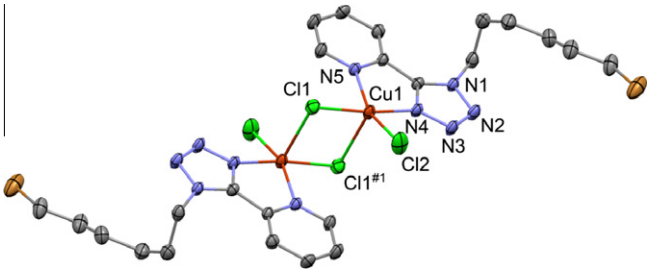

Fig. 1. Molecular structure of **1** with displacement ellipsoids at the 50% probability level (H atoms omitted). The complex lies on a crystallographic inversion centre.

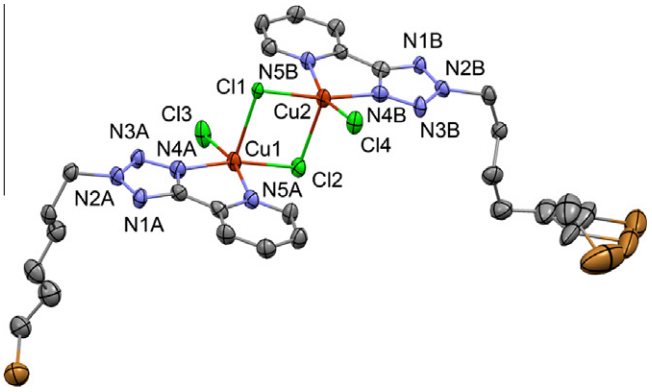

Fig. 2. Molecular structure of **2** with displacement ellipsoids at the 50% probability level (H atoms omitted). One bromohexyl pendant arm is modelled as disordered over three orientations.

Table 2
Selected bond lengths (Å) and angles (°) for **1**.

Cu(1)–Cl(1)	2.2553(7)	Cu(1)–N(4)	1.987(2)
Cu(1)–Cl(1)$^{\#1}$	2.6392(8)	Cu(1)–N(5)	2.088(2)
Cu(1)–Cl(2)	2.2257(8)		
Cl(1)–Cu(1)–Cl(2)	94.32(3)	N(4)–Cu(1)–Cl(1)	172.29(7)
Cu(1)–Cl(1)–Cu(1)$^{\#1}$	89.97(2)	N(4)–Cu(1)–Cl(2)	92.38(7)
Cl(2)–Cu(1)–Cl(1)$^{\#1}$	106.12(3)	N(4)–Cu(1)–Cl(1)$^{\#1}$	91.82(7)
N(5)–Cu(1)–Cl(1)	94.28(6)	N(4)–Cu(1)–N(5)	78.19(9)
N(5)–Cu(1)–Cl(2)	160.64(7)	Cl(1)–Cu(1)–Cl(1)$^{\#1}$	90.03(2)
N(5)–Cu(1)–Cl(1)$^{\#1}$	91.20(6)		

Symmetry code #1: $2-x, -y, -z$.

Table 3
Selected bond lengths (Å) and angles (°) for **2**.

Cu(1)–Cl(3)	2.235(2)	Cu(2)–Cl(4)	2.229(2)
Cu(1)–Cl(1)	2.716(2)	Cu(2)–Cl(2)	2.671(2)
Cu(1)–Cl(2)	2.2637(19)	Cu(2)–Cl(1)	2.3178(18)
Cu(1)–N(4A)	2.012(6)	Cu(2)–N(4B)	2.013(6)
Cu(1)–N(5A)	2.085(6)	Cu(2)–N(5B)	2.090(6)
Cl(3)–Cu(1)–Cl(2)	93.87(8)	Cl(4)–Cu(2)–Cl(1)	94.10(7)
Cl(2)–Cu(1)–Cl(1)	92.36(7)	Cl(1)–Cu(2)–Cl(2)	92.30(7)
Cl(3)–Cu(1)–Cl(1)	101.41(8)	Cl(4)–Cu(2)–Cl(2)	104.93(8)
N(4A)–Cu(1)–Cl(3)	91.79(19)	N(4B)–Cu(2)–Cl(4)	90.89(18)
N(4A)–Cu(1)–Cl(2)	167.9(2)	N(4B)–Cu(2)–Cl(1)	169.71(19)
N(4A)–Cu(1)–Cl(1)	97.0(2)	N(4B)–Cu(2)–Cl(2)	95.09(19)
N(4A)–Cu(1)–N(5A)	78.5(2)	N(4B)–Cu(2)–N(5B)	78.5(2)
N(5A)–Cu(1)–Cl(1)	91.24(19)	N(5B)–Cu(2)–Cl(1)	94.41(17)
N(5A)–Cu(1)–Cl(2)	93.66(18)	N(5B)–Cu(2)–Cl(2)	90.10(19)
N(5A)–Cu(1)–Cl(3)	165.0(2)	N(5B)–Cu(2)–Cl(4)	162.39(19)
Cu(2)–Cl(1)–Cu(1)	86.57(6)	Cu(1)–Cl(2)–Cu(2)	88.75(7)

Table 4
Selected bond lengths (Å) and angles (°) for **3**.

Co(1)–N(4)	2.142(3)	Co(1)–N(4A)	2.122(3)
Co(1)–N(5)	2.139(3)	Co(1)–N(5A)	2.144(3)
Co(1)–N(6)	2.039(3)	Co(1)–N(6A)	2.082(3)
N(6)–Co(1)–N(6A)	178.22(13)	N(6)–Co(1)–N(4A)	94.33(12)
N(6A)–Co(1)–N(4A)	87.44(12)	N(6)–Co(1)–N(5)	90.03(12)
N(6A)–Co(1)–N(5)	89.80(12)	N(4A)–Co(1)–N(5)	103.13(12)
N(6)–Co(1)–N(4)	93.09(12)	N(6A)–Co(1)–N(4)	85.14(12)
N(4A)–Co(1)–N(4)	172.57(12)	N(5)–Co(1)–N(4)	76.56(12)
N(6)–Co(1)–N(5A)	91.55(12)	N(6A)–Co(1)–N(5A)	88.62(12)
N(4A)–Co(1)–N(5A)	76.73(11)	N(5)–Co(1)–N(5A)	178.41(12)
N(4)–Co(1)–N(5A)	103.37(11)		

Table 5
Selected bond lengths (Å) and angles (°) for **4**.

Co(1A)–N(6A)	2.080(7)	Co(1B)–N(6B)	2.061(9)
Co(1A)–N(4A)	2.142(6)	Co(1B)–N(4B)	2.137(7)
Co(1A)–N(5A)	2.158(6)	Co(1B)–N(5B)	2.156(6)
N(6A)–Co(1A)–N(4A)	92.4(3)	N(6B)–Co(1B)–N(4B)	88.6(3)
N(6A)$^{\#1}$–Co(1A)–N(4A)	87.6(3)	N(6B)–Co(1B)–N(4B)$^{\#2}$	91.4(3)
N(6A)–Co(1A)–N(5A)	92.1(2)	N(6B)$^{\#2}$–Co(1B)–N(5B)	87.4(3)
N(6A)–Co(1A)–N(5A)$^{\#1}$	87.9(2)	N(6B)–Co(1B)–N(5B)	92.6(3)
N(4A)–Co(1A)–N(5A)	76.7(2)	N(4B)$^{\#2}$–Co(1B)–N(5B)	102.8(2)
N(4A)–Co(1A)–N(5A)$^{\#1}$	103.3(2)	N(4B)–Co(1B)–N(5B)$^{\#2}$	77.2(2)

Symmetry code #1: $-x, -y, -z$, #2: $1-x, -y, 1-z$.

apparatus and are uncorrected. Mass spectra were collected in the Mass Spectrometry unit in the Centre for Synthesis and Chemical Biology, University College, Dublin. Magnetic susceptibility measurements were carried out at room temperature using a Johnson Matthey Magnetic Susceptibility Balance with $[HgCo(SCN)_4]$ as reference. Microanalyses were carried out at the Microanalytical Laboratory of University College, Dublin. Standard Schlenk techniques were used throughout. Starting materials were commercially obtained and used without further purification. *Caution!* Nitrogen-rich compounds such as tetrazole derivatives are used as components for explosive mixtures [1]. In our laboratory, the reactions described were run on a few gram scale, and no problems were encountered. However, great caution should be exercised when heating or handling compounds of this type. *Caution!* Although not encountered in our experiments, perchlorate salts of metal ions are potentially explosive and should be manipulated with care and used only in small quantities.

3.1. Synthesis of 2-(2H-tetrazol-5-yl)pyridine (*L1*)

A suspension of 2-cyanopyridine (4.14 g, 40 mmol), sodium azide (5.72 g, 88 mmol), ammonium chloride (4.70 g, 88 mmol) and lithium chloride (1.20 g, 28 mmol) in anhydrous dimethylformamide (40 mL) was stirred for 10 h at 110 °C. After this time, the solution was cooled and the insoluble salts were removed by filtration. The solvent was then evaporated under reduced pressure and the residue was dissolved in deionised water (200 mL) and acidified with concentrated HCl (3 mL), to initiate precipitation. The product was removed by filtration, washed with water (3×40 mL) and dried to give a brown solid. This was recrystallised from hot ethanol to afford **L1** as brown needles (3 g, yield 51.3%). M.p. 221–223 °C. *Anal.* Calc. for $C_6H_5N_5$ (147.14): C, 48.98; H, 3.42; N, 47.60. Found: C, 48.97; H, 3.44; N, 47.61%. ^{1}H NMR (CD_3OD): $\delta = 8.76$ (d, 1H, $J = 7.9$ Hz, pyr-H), 8.25 (d, 1H, $J = 7.9$ Hz, pyr-H), 8.03 (t, 1H, $J = 7.9$ Hz, pyr-H), 7.56 (t, 1H, $J = 7.9$ Hz, pyr-H), 3.9 (s, 1H, tet-H) ppm. ^{13}C NMR (CD_3OD): $\delta = 154.9$ (CN_4), 150.1, 143.7, 138.3, 126.2, 122.7 ppm. ESI-HRMS: calc. for $C_6H_5N_5$ $[M]^+$ 147.054, found 147.054.

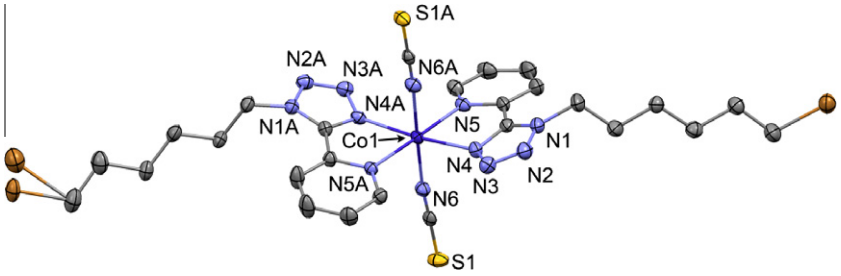

Fig. 3. Molecular structure of **3** with displacement ellipsoids at the 50% probability level (H atoms omitted). One bromohexyl pendant arm displays disorder.

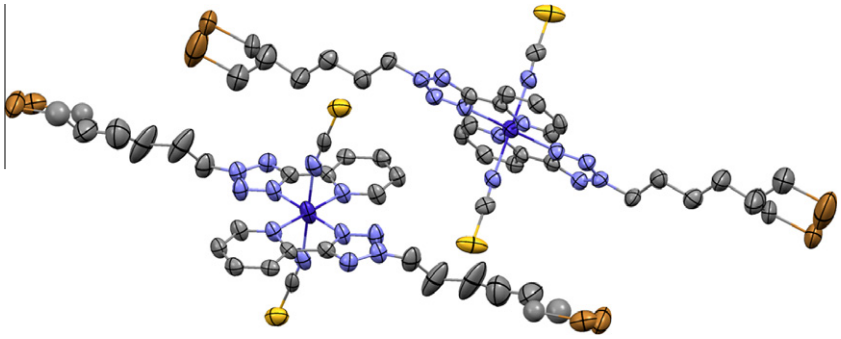

Fig. 4. Molecular structure of **4** with displacement ellipsoids at the 50% probability level (H atoms omitted). Two independent complexes lie on crystallographic inversion centres. Both display disorder of the bromohexyl pendant arms.

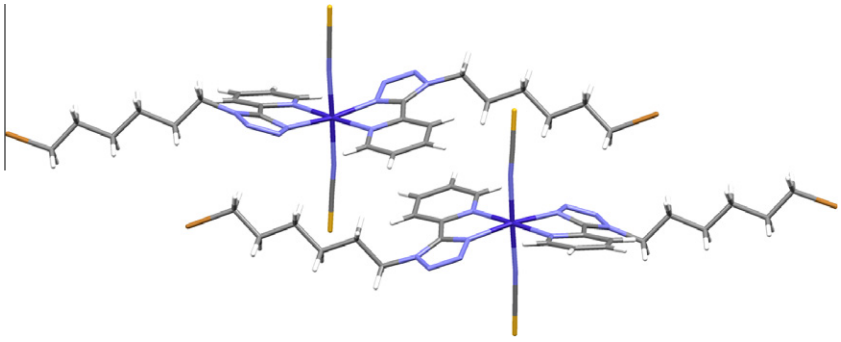

Fig. 5. Neighbouring complexes in the crystal structure of **3**. In the centre, the face-to-face interaction between pyridyl–tetrazole ligands with the smaller degree of twist is visible. On the left and right sides, the tetrazole rings are twisted away from the planes of the pyridyl rings in order to accommodate the neighbouring bromohexyl chains.

Table 6
Selected bond lengths (Å) and angles (°) for **5**.

Fe(1)–O(1W)	2.122(3)	Fe(1)–N(5)	2.198(3)
Fe(1)–N(4)	2.141(3)	C(12)–Br(1)	1.947(4)
O(1W)–Fe(1)–N(4)	88.10(11)	O(1W)–Fe(1)–N(4)$^{\#1}$	91.90(11)
O(1W)$^{\#1}$–Fe(1)–N(5)	89.46(10)	O(1W)–Fe(1)–N(5)	90.54(10)
N(4)–Fe–N(5)	75.03(11)	N(4)$^{\#1}$–Fe(1)–N(5)	104.97(11)

Symmetry code #1: $-x, -y, -z$.

3.2. Synthesis of 2-(6″-bromohexyl)-(1-tetrazol-5-yl)pyridine (*L2*) and 2-(6″-bromohexyl)-(2-tetrazol-5-yl)pyridine (*L3*)

To **L1** (1 g, 6.8 mmol) dissolved in either acetonitrile or 2-butanone (30 mL) was added potassium carbonate (9.38 g, 68 mmol). The resulting solution was refluxed for 30 min and to the hot solution was added 1,6-dibromohexane (4.97 g, 24 mmol). The reaction mixture was then stirred at reflux temperature for a further 24 h. After cooling, the solvent was removed under reduced pressure to afford an oil, which was purified by column chromatography on silica gel (initially at a ratio of petroleum ether:ethyl acetate 80:20, followed by the ratio of 60:40). This gave the products **L2** and **L3**.

L2: Waxy white solid (0.55 g, yield 26%). M.p. 39–41 °C. *Anal.* Calc. for $C_{12}H_{16}N_5Br$ (310.19): C, 46.46; H, 5.20; N, 22.58. Found: C, 46.50; H, 5.17; N, 22.62%. ^{1}H NMR ($CDCl_3$): δ = 8.77 (d, 1H, J = 7.5 Hz, pyr-H), 8.37 (d, 1H, J = 7.5 Hz, pyr-H), 7.96 (t, 1H, J = 7.5 Hz, pyr-H), 7.52 (t, 1H, J = 7.5 Hz, pyr-H), 5.00 (t, 2H, J = 6.9 Hz, CH_2N), 3.42 (t, 2H, J = 6.9 Hz, CH_2Br), 2.02 (q, 2H, J = 7.1 Hz, CH_2), 1.87 (m, 2H, CH_2), 1.48 (m, 4H, CH_2) ppm. ^{13}C NMR ($CDCl_3$): δ = 151.4 (CN_4), 149.3, 144.6, 137.1, 125.1, 124.2, 49.2 (CH_2N), 33.5 (CH_2Br), 32.3, 32.1, 29.4, 27.2 ppm. ESI-HRMS: calc. for $C_{12}H_{17}BrN_5$ $[M+1]^+$ 310.067, found 310.068.

L3: Waxy white solid (0.35 g, yield 17%). M.p. 36–38 °C. *Anal.* Calc. for $C_{12}H_{16}N_5Br$ (310.19): C, 46.46; H, 5.20; N, 22.58. Found: C, 46.44; H, 5.17; N, 22.63%. ^{1}H NMR ($CDCl_3$): δ = 8.80 (d, 1H, J = 7.7 Hz, pyr-H), 8.27 (d, 1H, J = 7.7 Hz, pyr-H), 7.90 (t, 1H, J = 7.7 Hz, pyr-H), 7.43 (t, 1H, J = 7.7 Hz, pyr-H), 4.73 (t, 2H, J = 6.8 Hz, CH_2N), 3.39 (t, 2H, J = 6.8 Hz, CH_2Br), 2.13 (q, 2H, J = 6.8 Hz, CH_2), 1.83 (m, 2H, CH_2), 1.51 (m, 4H, CH_2) ppm. ^{13}C

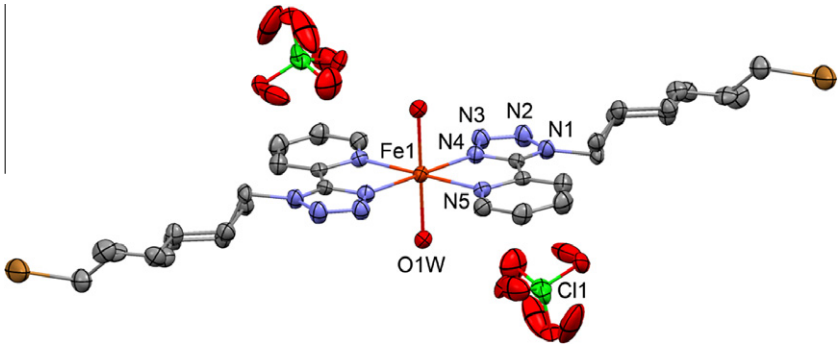

Fig. 6. Molecular structure of **5** with displacement ellipsoids at the 50% probability level (H atoms omitted). The complex lies on a crystallographic inversion centre. The bromohexyl chains and the perchlorate anions are modelled as disordered.

NMR ($CDCl_3$): δ = 164.7 (CN_4), 150.2, 146.7, 137.1, 124.8, 122.3, 53.2 (CH_2N), 33.4 (CH_2Br), 32.4, 32.2, 29.0, 27.3 ppm. ESI-HRMS: calc. for $C_{12}H_{17}BrN_5$ $[M+1]^+$ 310.067, found 310.066.

3.3. General coordination reactions (**1**–**6**)

The appropriate tetrazole ligand, **L2** or **L3** (0.20 g, 1.36 mmol), was dissolved in methanol (30 mL) and was added to a solution of the appropriate metal salt (1.36 mmol) in methanol (25 mL). The resulting strongly-coloured solution was then heated to reflux for 2 h before being allowed to stand at room temperature for several days.

3.3.1. $[Cu(L2)Cl_2]_2$ (**1**)

Dark green crystals (0.137 g, yield 49%). *Anal.* Calc. for $C_{24}H_{32}Br_2Cl_4Cu_2N_{10}$ (889.29): C, 32.41; H, 3.63; N, 15.75. Found: C, 32.52; H, 3.71; N, 15.73%. IR (KBr): υ = 2923, 2852, 1648, 1610, 1482, 1256, 1167, 1139, 1019, 803, 723 cm^{-1}. λ_{max} (CH_3CN) 832 nm, ε = 93 M^{-1} cm^{-1}. Magnetic moment: 2.6 BM.

3.3.2. $[Cu(L3)Cl_2]_2$ (**2**)

Dark green crystals (0.14 g, yield 50%). *Anal.* Calc. for $C_{24}H_{32}Br_2Cl_4Cu_2N_{10}$ (889.29): C, 32.41; H, 3.63; N, 15.75. Found: C, 32.42; H, 3.51; N, 15.78%. IR (KBr): υ = 2923, 2856, 1648, 1610, 1483, 1278, 1165, 1019, 803, 721 cm^{-1}. λ_{max} (CH_3CN) 812 nm, ε = 55 M^{-1} cm^{-1}. Magnetic moment: 3.2 BM.

3.3.3. $Co(L2)_2(NCS)_2$ (**3**)

Rust coloured crystals (0.130 g, yield 26%). *Anal.* Calc. for $C_{26}H_{32}Br_2CoN_{12}S_2$ (795.48): C, 39.26; H, 4.05; N, 21.13. Found: C, 39.31; H, 4.09; N, 21.18%. IR (KBr): υ = 2933, 2861, 2075, 1648, 1473, 1368, 1247, 1159, 1105, 1047, 795, 728 cm^{-1}. λ_{max} (CH_3CN) 512 nm, ε = 37 M^{-1} cm^{-1}. Magnetic moment: 4.5 BM.

3.3.4. $Co(L3)_2(NCS)_2$ (**4**)

Green crystals (0.146 g, yield 29%). *Anal.* Calc. for $C_{26}H_{32}Br_2CoN_{12}S_2$ (795.48): C, 39.26; H, 4.05; N, 21.13. Found: C, 39.65; H, 4.19; N, 20.86%. IR (KBr): υ = 2928, 2858, 2075, 1654, 1474, 1368, 1247, 1159, 1105, 1047, 796, 728 cm^{-1}. λ_{max} (CH_3CN) 512 nm, ε = 45 M^{-1} cm^{-1}. Magnetic moment: 3.65 BM.

3.3.5. $[Fe(L2)_2(H_2O)_2](ClO_4)_2$ (**5**)

Yellow crystals (0.09 g, yield 16%). *Anal.* Calc. for $C_{24}H_{36}Br_2Cl_2FeN_{10}O_{10}$ (911.16): C, 31.64; H, 3.98; N, 15.37. Found: C, 31.62; H, 3.91; N, 15.41%. IR (KBr): υ = 3407, 2924, 2852, 1637, 1478, 1379, 1250, 1143, 1112, 798, 727 cm^{-1}. λ_{max} (CH_3CN) 364 nm, ε = 1718 M^{-1} cm^{-1}. Magnetic moment: 4.7 BM.

3.3.6. $[Fe(L3)_2(H_2O)_2](ClO_4)_2$ (**6**)

Yellow solid (0.11 g, yield 20%). *Anal.* Calc. for $C_{24}H_{36}Br_2Cl_2FeN_{10}O_{10}$ (911.16): C, 31.64; H, 3.98; N, 15.37. Found: C, 31.59; H, 3.98; N, 15.48%. IR (KBr): υ = 3410, 2942, 2862, 1638, 1451, 1384, 1145, 1117, 1089, 731 cm^{-1}. λ_{max} (CH_3CN) 348 nm, ε = 219 M^{-1} cm^{-1}. Magnetic moment: 5.0 BM. To date, we have not been able to obtain crystals of **6** suitable for X-ray diffraction analysis.

3.4. Crystallography

X-ray diffraction data were collected on a Bruker APEX-II CCD diffractometer using graphite-monochromated Mo Kα radiation (λ = 0.7107 Å). In each case, a multi-scan correction was applied and the structures were refined against F^2 using all reflections [23]. All non-H atoms were refined with anisotropic atomic displacement parameters and H atoms were placed at calculated positions and refined using a riding model. One of the hexyl chains in **2** is disordered, and the terminal CH_2Br unit was refined over three orientations with site occupancies of 0.40, 0.40 and 0.20. Similarity restraints were applied to the bond distances and to the displacement parameters. For **3**, one of the Br atoms appears to be disordered and was included in two positions with refined site occupancies 0.81(1):0.19(1). Corresponding disorder of the neighbouring CH_2 group could not be resolved, so one of the Br positions lies ca. 2.3 Å from the CH_2 group. Comparable results were obtained from full data collections for two crystals within the batch. In **4**, both independent bromohexyl chains are modelled as disordered over two orientations, one with site occupancies 0.50:0.50 and one with 0.70:0.30. Similarity restraints were applied to the bond distances and to the displacement parameters. In **5**, the bromohexyl chain is modelled over two orientations with site occupancies 0.50:0.50, and the perchlorate anion is also modelled as disordered. The H atoms of the coordinated water molecules were visible in difference Fourier maps and their positions were refined with restrained O–H distances.

4. Conclusions

The X-ray structures of several M(II) complexes of 2-(2H-tetrazol-5-yl)pyridine derivatives, containing a 6-bromohexyl pendant arm at either the *1-N* (**L2**) or *2-N* (**L3**) position of the tetrazole ring, have been studied. In all cases, the 5-(2-pyridyl)tetrazole ligand coordinates in a bidentate fashion through the pyridine N atom and the *1-N* atom of the tetrazole ring to form a five-membered chelate ring with the metal ion. The coordination geometries in the two Cu(II) complexes (**1** and **2**) are slightly distorted square-pyramidal, due mainly to the formation of a dimeric Cu_2Cl_2 core. The coordination geometry at the metal centres in the other three

structures (**3**, **4** and **5**) can be described as slightly distorted octahedral, with two 5-(2-pyridyl)tetrazole ligands occupying the equatorial plane in all cases. The axial positions are occupied by the two thiocyanate anions in the Co(II) complexes, while they are occupied by two water molecules in the case of the Fe(II) complex. The biological studies of these complexes and complexes involving other first row transition metal ions will be published in a separate paper [17].

Acknowledgments

J.G. thanks the Postgraduate R&D Skills programme (Technological Sector Research, Strand I) and IT Tallaght Dublin for financial assistance. U.S. thanks NUIM for a John & Pat Hume Fellowship. A.D.B. is grateful to the Danish Natural Sciences Research Council and the Carlsberg Foundation for provision of the X-ray equipment.

Appendix A. Supplementary data

CCDC 827225, 759312, 827226, 759313 and 759314 contain the supplementary crystallographic data for **1**–**5**. These data can be obtained free of charge via http://www.ccdc.cam.ac.uk/conts/retrieving.html, or from the Cambridge Crystallographic Data Centre, 12 Union Road, Cambridge CB2 1EZ, UK; fax: (+44) 1223-336-033; or e-mail: deposit@ccdc.cam.ac.uk. Supplementary data associated with this article can be found, in the online version, at doi:10.1016/j.poly.2011.11.038.

References

[1] R.N. Butler, in: A.R. Katritzky, C.W. Rees, E.F.V. Scriven (Eds.), Comprehensive Heterocyclic Chemistry II, vol. 4, Pergamon, Oxford, 1996, p. 621.
[2] R.J. Herr, Bioorg. Med. Chem. 10 (2002) 3379.
[3] J. McGinley, A. Fleming, J. Inclusion Phenom. Macrocycl. Chem. 61 (2008) 1.
[4] G. Aromí, L.A. Barrios, O. Roubeau, P. Gamez, Coord. Chem. Rev. 255 (2011) 485.
[5] (a) Z.P. Demko, K.B. Sharpless, J. Org. Chem. 66 (2001) 7945;
(b) F. Himo, Z.P. Demko, L. Noodleman, K.B. Sharpless, J. Am. Chem. Soc. 125 (2003) 9983.
[6] T. Mavromoustakos, A. Kolocouris, M. Zervou, P. Roumelioti, J. Matsoukas, R. Weisemann, J. Med. Chem. 42 (1999) 1714.
[7] (a) R.A. Powers, B.K. Shoichet, J. Med. Chem. 45 (2002) 3222;
(b) S.Y. Kang, S.-H. Lee, H.J. Seo, M.E. Jung, K. Ahn, J. Kim, J. Lee, Bioorg. Med. Chem. Lett. 18 (2008) 2385.
[8] (a) G.C.G. Pais, X. Zhang, C. Marchand, N. Neamati, K. Cowansage, E.S. Svarovskaia, V.K. Pathak, Y. Tang, M. Nicklaus, Y. Pommier, T.R. Burke Jr., J. Med. Chem. 45 (2002) 3184;
(b) B.C.H. May, A.D. Abell, J. Chem. Soc., Perkin Trans. 1 (2002) 172.
[9] (a) P. Lin, W. Clegg, R.W. Harrinton, R.A. Henderson, Dalton Trans. (2005) 2388;
(b) W. Zhang, F. Zhao, T. Liu, M. Yuan, Z.-M. Wang, S. Gao, Inorg. Chem. 46 (2007) 2541;
(c) S. Stagni, E. Orselli, A. Palazzi, L. De Cola, S. Zacchini, C. Femoni, M. Marcaccio, F. Paolucci, S. Zanarini, Inorg. Chem. 46 (2007) 9126;
(d) G.-W. Yang, Q.-Y. Li, Y. Zhou, P. Sha, Y.-S. Ma, R.-X. Yuan, Inorg. Chem. Commun. 11 (2008) 723;
(e) S. Stagni, S. Colella, A. Palazzi, G. Valenti, S. Zacchini, F. Paolucci, M. Marcaccio, R.Q. Albuquerque, L. De Cola, Inorg. Chem. 47 (2008) 10509;
(f) A. Białońska, R. Bronisz, Tetrahedron 64 (2008) 9771;
(g) B. Liu, Y.-C. Qiu, G. Peng, L. Ma, L.-M. Jin, J.-B. Cai, H. Deng, Inorg. Chem. Commun. 12 (2009) 1200;
(h) Q.-Y. Li, G.-W. Yang, X.-Y. Tang, Y.-S. Ma, F. Zhou, W. Liu, J. Chen, H. Zhou, Inorg. Chem. Commun. 13 (2010) 254;
(i) T. Hu, L. Liu, X. Lv, X. Chen, H. He, F. Dai, G. Zhang, D. Sun, Polyhedron 29 (2010) 296;
(j) Y. Qiu, B. Liu, G. Peng, J. Cai, H. Deng, M. Zeller, Inorg. Chem. Commun. 13 (2010) 749;
(k) Y. Huang, L.-Z. Chen, R.-G. Xiong, X.-Z. You, Inorg. Chim. Acta 363 (2010) 2512;
(l) J.M. Seco, M. de Araújo Farias, N.M. Bachs, A.B. Caballero, A. Salinas-Castillo, A. Rodríguez-Diéguez, Inorg. Chim. Acta 363 (2010) 3194;
(m) B.K. Tripuramallu, R. Kishore, S.K. Das, Inorg. Chim. Acta 368 (2011) 132.
[10] (a) X. He, C.-Z. Lu, D.-Q. Yuan, Inorg. Chem. 45 (2006) 5760;
(b) H. Zhao, Z.-R. Qu, H.-Y. Ye, R.-G. Xiong, Chem. Soc. Rev. 37 (2008) 84.
[11] A. Fleming, J. Gaire, F. Kelleher, J. McGinley, V. McKee, Tetrahedron 67 (2011) 3260.
[12] A.D. Bond, A. Fleming, J. Gaire, F. Kelleher, J. McGinley, V. McKee, Tetrahedron 65 (2009) 7942.
[13] A.D. Bond, A. Fleming, F. Kelleher, J. McGinley, V. Prajapati, S. Skovsgaard, Tetrahedron 63 (2007) 6835.
[14] A.D. Bond, A. Fleming, F. Kelleher, J. McGinley, V. Prajapati, Tetrahedron 62 (2006) 9577.
[15] A. Fleming, F. Kelleher, M.F. Mahon, J. McGinley, V. Prajapati, Tetrahedron 61 (2005) 7002.
[16] A.F.M. Fleming, F. Kelleher, M.F. Mahon, J. McGinley, K.C. Molloy, V. Prajapati, Acta Crystallogr., Sect. E 60 (2004) 2388.
[17] A. Fleming, J. Gaire, F. Kelleher, J. McGinley, U. Sheridan, unpublished results.
[18] H. Gallardo, R. Magnago, A.J. Bortoluzzi, Liq. Cryst. 28 (2001) 1343.
[19] P.A. Bethel, M.S. Hill, M.F. Mahon, K.C. Molloy, J. Chem. Soc., Perkin Trans. 1 (1999) 3507.
[20] R.N. Butler, A.F.M. Fleming, J. Heterocycl. Chem. 34 (1997) 691.
[21] A.W. Addison, T.N. Rao, J. Reedijk, J. Van Rijn, G.C. Verschoor, J. Chem. Soc., Dalton Trans. (1984) 1349.
[22] (a) See, for example M.F. Mahon, J. McGinley, A.D. Rooney, J.M.D. Walsh, Inorg. Chim. Acta 362 (2009) 2353;
(b) Y.-Y. Kou, J.-L. Tian, D.-D. Li, H. Liu, W. Gu, S.-P. Yan, J. Coord. Chem. 62 (2009) 2182;
(c) S. Mandal, F. Lloret, R. Mukherjee, Inorg. Chim. Acta 362 (2009) 27;
(d) D.H. Jeong, W.J. Park, J.H. Jeong, D.G. Churchill, H. Lee, Inorg. Chem. Commun. 11 (2008) 1170;
(e) J. Astner, M. Weitzer, S.P. Foxon, S. Schindler, F.W. Heinemann, J. Mukherjee, R. Gupta, V. Mahadevan, R. Mukherjee, Inorg. Chim. Acta 361 (2008) 279;
(f) A. Bernalte-García, A.M. Lozano-Vila, F. Luna-Giles, R. Pedrero-Marín, Polyhedron 25 (2006) 1399;
(g) E. Tynan, P. Jensen, A.C. Lees, B. Moubaraki, K.S. Murray, P.E. Kruger, CrystEngComm 7 (2005) 90.
[23] G.M. Sheldrick, Acta Crystallogr., Sect. A 64 (2008) 112.